Front. Chem. Sci. Eng. 2014, 8(4): 478–487
DOI 10.1007/s11705-014-1453-7

RESEARCH ARTICLE

Effect of triethylamine treatment of titanium silicalite-1 on propylene epoxidation

Juan XU, Yaquan WANG (✉), Wenping FENG, Yi LIN, Shuhai WANG

Key Laboratory for Green Chemical Technology of the Ministry of Education, School of Chemical Engineering & Technology,
Tianjin University, Tianjin 300072, China

Abstract Titanium silicalite-1(TS-1) treated with triethylamine (TEA) solution under different conditions was characterized by X-ray powder diffraction (XRD), Fourier-transform infrared spectrum (FTIR), ultraviolet-visible diffuse reflectance spectrum (UV-Vis), nitrogen physical adsorption and desorption, scanning electron microscopy (SEM) and transmission electron microscopy (TEM). The characterization results show that many irregular hollows are generated in the TS-1 crystals due to the random dissolution of framework silicon and the volume of the hollow cavities increase with increasing the TEA concentration, and the treatment temperature and time. The modified TS-1 samples improved in varying degrees the catalyst life for the epoxidation of propylene in a fixed-bed reactor probably due to the generation of the hollows to make it easy for the reactants and products to diffuse out of the channels.

Keywords titanium silicalite-1, triethylamine, hollow cavity, epoxidation of propylene, catalyst life

1 Introduction

Propylene oxide (PO) is an important chemical product and has been widely used in the production of polyether polyols, propylene glycol, propylene glycol ethers, etc. [1]. Currently, PO is mainly produced by the chlorohydrin process or hydroperoxide process. However, the chlorohydrin process suffers from serious environmental and safety drawbacks due to the utilization of environmentally hazardous chlorine and the production of chlorinated organic by-products. The hydroperoxide process uses tert-butyl hydroperoxide to oxidize propene with the major shortcoming being the generation of the large quantities of co-products such as tert-butyl alcohol, which may represent up to three times the PO production and cause serious economic problems [2,3]. Consequently, a short and clean process for producing PO is highly desirable, and a great deal of effort has been put into the catalytic epoxidation of propylene to PO in the past two decades.

Since titanium silicalite-1 (TS-1) was invented by Taramasso et al. [4] in 1983, it has attracted much attention for its excellent catalytic performance in the selective oxidation of various organic compounds with dilute H_2O_2 as oxidant under mild conditions, such as the oxidation of alkanes, the epoxidation of alkenes, the hydroxylation of aromatics, and the ammoxidation of ketones [5–11]. The invention of TS-1 also opened a new route for the manufacture of PO. The direct epoxidation of propylene to PO over TS-1 using hydrogen peroxide as the oxidant is regarded as an important development trend of PO green production for its mild reaction conditions, high catalytic activity and high atom economy [12–18]. However, the application of TS-1 as catalyst suffers from diffusional limitation on the reaction due to the size of the zeolite channels (0.56 nm × 0.53 nm) [19]. In order to overcome this problem, several approaches have been developed to introduce mesopores and macropores into zeolite. It has been demonstrated that the post-chemical treatment by a basic solution is an effective way to generate hollow cavities [20–23]. Lin and coworkers [24,25] have prepared the catalyst called HTS-1 with hollow cavities by the post treatments firstly with an acid and then with an organic base, and found that the catalyst stability can be improved in the ammoximation of cyclohexanone. Tuel and coworkers [26] have obtained a TS-1 zeolite with hollow structure by treatment with tetrapropyl ammonium hydroxide (TPAOH) and found that its catalytic activity is considerably improved in the hydroxylation of phenol.

Received July 1, 2014; accepted September 6, 2014

E-mail: yqwang@tju.edu.cn

Other groups [19,27–28] have also reported that TPAOH is an effective agent to create hollow cavities in TS-1. However, TPAOH is very expensive and cannot be recycled.

In this contribution, we describe a method to obtain the hollow TS-1 through the treatment with cheap triethylamine (TEA), which has been rarely reported. The triethylamine can be recycled after the treatment through simple distillation from the treatment solution. The catalyst life of the modified TS-1 samples in the epoxidation of propylene to PO is significantly improved.

2 Experimental

2.1 Materials

Tetraethyl orthosilicate (TEOS, AR), tetrabutyl titanate (TBOT, AR), methanol (AR), isopropyl alcohol (IPA, AR), triethylamine (AR) and 30 wt-% hydrogen peroxide (AR) were purchased from Tianjin Guang Fu Fine Chemical Research Institute Co., Ltd., China. Propylene (99.99%) was purchased from Tianjin Division of SINOPEC. LUDOX As-40 colloidal silica (40 wt-% suspension in water) was purchased from Sigma-Aldrich. Tetrapropyl ammonium hydroxide was prepared through ion-exchange. The preparation of TS-1 (Si/Ti = 70, mole ratio) were described in our previous work [29].

2.2 Treatment of TS-1 with TEA

TS-1 (5 g) was added into the TEA solution with different concentrations in a 100 cm^3 PTFE lined stainless-steel autoclave. After the mixture was vigorously stirred for 5 min, the autoclave was heated to the predetermined temperature and kept at this temperature for a predetermined time under static conditions. Then the autoclave was rapidly cooled to room temperature and the treated TS-1 was obtained after centrifuged, washed with deionized water, dried at 393 K for 8 h, and finally calcined at 823 K for 6 h in air. The catalysts are labeled as TS-1-x-y-z, where x denotes the concentration of TEA in the treatment solution (0.15, 0.30, 0.60, and 1.20 $mol \cdot L^{-1}$), y denotes the treatment temperature (433, 443, and 453 K), and z denotes the treatment time (24, 48, 96, and 144 h). The untreated TS-1 is denoted as TS-1-null.

2.3 Preparation of TS-1/SiO_2

TS-1/SiO_2 was prepared by grinding 2.5 g 40 wt-% silica sol, 5 g TS-1 powder and 0.20 g Sesbania cannabina Pers powder for 30 min, and then extrudating into Φ1 mm strips. The strips were dried at 393 K for 6 h and calcined at 823 K for 6 h in air. The TS-1/SiO_2 strips were cut into cylindrical pieces of Φ1 mm × 1 mm for the use in the fixed-bed reactor.

2.4 Characterization of TS-1samples

X-ray powder diffraction (XRD) patterns were obtained on a Rigaku D/max 2500 diffractometer using Cu Kα radiation (λ = 0.154 nm) with steps of 0.02° and a scanning rate of $8° \cdot min^{-1}$ in the 2θ ranges from 5° to 50°.

The Si and Ti contents of TS-1 samples were analyzed by PerkinElmer Optima 2100 DV inductive coupling plasma spectrometer (ICP).

Transmission electron microscopy (TEM) images were recorded on a JEM-2010 FEF field emission electron microscope operating at 200 kV and scanning electron microscopy (SEM) images were recorded on a Nanosem 430 field emission scanning electron microscopy with an accelerating voltage of 5 kV.

N_2 adsorption/desorption isotherms were measured on a Micromeritics TriStar 3000 apparatus at 77 K. The specific surface areas, micropore volumes and volumes of the hollow cavities were calculated by BET equation, *t*-plot and BJH method (desorption), respectively.

Fourier-transform infrared (FTIR) spectra of the samples were recorded from 2000 to 400 cm^{-1} with a resolution of 4 cm^{-1} on a Bruker Vertex 7.0 spectrometer, using the KBr wafer technique.

UV-Visible diffuse reflectance spectra (UV-Vis) were obtained on a Hitachi U-3010 spectrometer employing pure $BaSO_4$ as the reference in the range of 190–410 nm.

2.5 Epoxidation of propylene

The catalyst (3.00 g, 5.10 cm^3) mixed with 2.90 cm^3 quartz sand particles were added into a stainless steel tube reactor of 408 mm long with internal diameter of 5 mm. The reaction temperature was controlled by a thermostatic circulating water bath, and the temperature difference along the reactor was less than 0.5 K. The reaction pressure was 2.5 MPa which was realized with N_2. The propylene was in liquid under this pressure. After the reaction pressure reached 2.5 MPa, the flow rate of N_2 was kept at 0.67 $cm^3 \cdot s^{-1}$. When the pressure and temperature reached to the reaction condition set, liquid propylene of 4.07×10^{-3} $cm^3 \cdot s^{-1}$ and mixed solution of $CH_3OH/H_2O_2/H_2O$ of 5.83×10^{-3} $cm^3 \cdot s^{-1}$ were introduced into the reactor by two micropumps, respectively. Sodium acetate was added into the solution of $CH_3OH/H_2O_2/H_2O$ to regulate the PO selectivity within 93%–95% through neutralizing the acid sites on TS-1 samples [30]. After the reaction, the products entered the condenser cooled to 275 K. During the reaction, the products were sampled at regular intervals of 30 min through two valves with a tank in between at the bottom of the apparatus without releasing the pressure.

2.6 Product analysis

The products of the reaction were analyzed on a gas chromatography (GC-HP 4890) equipped with a flame ionization detector (FID) and an OV-1701 (30 m × 0.25 mm × 0.33 μm) capillary column with nitrogen as the carrier gas. The unreacted H_2O_2 was determined by means of iodometric method. The conversion of H_2O_2 and the selectivity of PO were calculated based on the starting amount of H_2O_2 according to the following two equations, respectively.

$$X_{H_2O_2} = \frac{n^0_{H_2O_2} - n_{H_2O_2}}{n^0_{H_2O_2}} \times 100\%, \tag{1}$$

$$S_{PO} = \frac{n_{PO}}{n_{PO} + n_{MME} + n_{PG}} \times 100\%. \tag{2}$$

MME and PG denote propylene glycol monomethyl ethers (with the two isomers combined together) and propylene glycol, respectively. $X_{H_2O_2}$ and S_{PO} denote the conversion of H_2O_2 and the selectivity of PO, respectively. n^0 and n represent the initial and the final amounts in moles, respectively. A lower $X_{H_2O_2}$has no economical feasibility for the industrial production of propylene oxide. So we regard the online reaction time of $X_{H_2O_2}$ above 95% as the catalyst life in our experiments.

3 Results and discussion

3.1 Characterization of TS-1 before and after TEA treatment

The X-ray powder diffraction patterns of TS-1 before and after TEA treatment are shown in Fig. 1. All the XRD patterns show similar characteristic peaks at $2\theta = 7.9°$, 8.9°, 23.1°, 23.9° and 24.4°, which correspond to the typical pattern of TS-1 [4,31]. The relative crystallinities, which were calculated by comparing the total intensity of the five characteristic peaks above with those of TS-1-null as 100%, are listed in Table 1. The results indicate that the relative crystallinities of all TS-1 samples after TEA treatment are lower than that of TS-1-null and decrease with increasing TEA concentrations (e.g., 97.3% to 76.1% *vs.* 0.15 to 1.2 mol·L^{-1}), treatment temperature e.g., 96.3% to 85.4% *vs.* 433 to 453 K) and time (e.g., 94.3% to 86.2% *vs.* 24 to 144 h). The samples treated with TEA can cause the dissolution of silica [21] and the dissolved silica is difficult to recrystallize because TEA cannot structurally direct the synthesis of the MFI topology and thus causes the decrease of the relative crystallinity [19]. The molar ratios of Si/Ti for all the samples are given in Table 1. It can be seen that these values of all the treated samples were lower than that of TS-1-null and decreased with increasing the TEA concentrations, the treatment temperature and time. The reason for this phenomenon is that treating TS-1 with TEA causes a loss of silicon and the amounts of lost silicon are different under different treatment conditions.

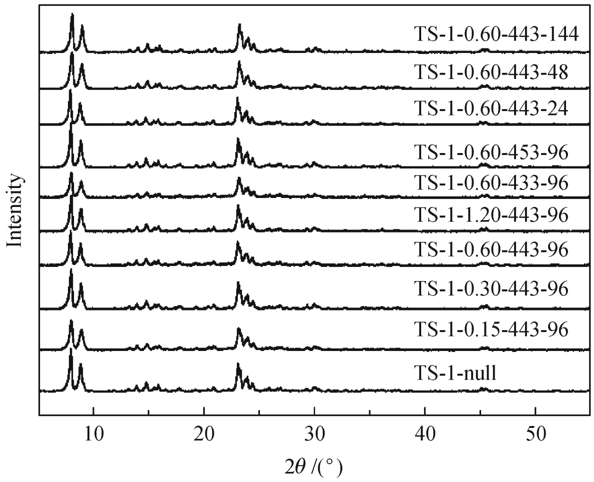

Fig. 1 XRD patterns of TS-1 samples before and after TEA treatment

The SEM images of TS-1 before and after treatment are given in Fig. 2. All the samples exhibit the same morphology of ellipsoids and have similar sizes of about 200 nm, agreeing with those of TS-1 crystals synthesized under the similar conditions in our previous work [29]. The results confirm that the samples treated with TEA do not influence the morphology or crystal size of TS-1.

The TEM images of all TS-1 samples are shown in Fig. 3. It is seen that many irregular hollow cavities appear in all the treated samples, whereas no cavity is observed in the TS-1-null sample. There are small hollow cavities in the sample when TS-1 is treated with a lower TEA concentration of 0.15 mol·L^{-1}. With increasing the TEA concentrations from 0.15 to 1.20 mol·L^{-1}, some small cavities merge together to generate the large hollow cavities. It is also seen that the sizes of the hollow cavities increases in varying degrees with increasing the treatment temperature and extending the treatment time.

The nitrogen adsorption-desorption isotherms of TS-1 samples before and after the TEA treatment are given in Fig. 4. It can be seen that, for the TS-1-null sample there is a low adsorption at low relative pressures ($p/p_0 < 0.9$), which is consistent with its microporous structure. The hysteresis loop at $p/p_0 > 0.9$ can be attributed to the condensation within the voids formed between the zeolitic particles [32]. The treated TS-1 samples exhibit type IV isotherm with an obvious hysteresis loop at relative pressure of p/p_0 between 0.4 and 1 in isotherms, which confirm the existence of large cavities in the crystal caused by the treatment of TEA.

The BET specific surface areas, micropore volumes and volumes of hollow cavities of these samples are listed in Table 1. The BET specific surface areas of the treated samples decrease slightly and the volumes of the hollow cavities increase appreciably compared with those of TS-1-null. The results are in agreement with the treatment of TS-1 with TPAOH in the literature [26]. The micropore volumes of all samples have no significant difference. The

Table 1 Textural properties of TS-1 samples before and after TEA treatment[a)]

Samples	Relative crystallinity / %	Si/Ti	S_{BET} /($\mathrm{m^2 \cdot g^{-1}}$)	V_{micro} /($\mathrm{cm^3 \cdot g^{-1}}$)	V_{hollow} /($\mathrm{cm^3 \cdot g^{-1}}$)	I_{960}/I_{550}
TS-1-null	100	68.5	426	0.114	–	0.362
TS-1-0.15-443-96	97.3	67.6	405	0.113	0.236	0.343
TS-1-0.30-443-96	93.3	66.8	399	0.112	0.245	0.336
TS-1-0.60-443-96	88.3	65.6	396	0.112	0.265	0.324
TS-1-1.20-443-96	76.1	60.7	384	0.109	0.313	0.302
TS-1-0.60-433-96	96.3	66.5	410	0.115	0.256	0.345
TS-1-0.60-453-96	85.4	65.2	392	0.111	0.268	0.319
TS-1-0.60-443-24	94.3	67.1	406	0.113	0.248	0.347
TS-1-0.60-443-48	90.3	66.3	403	0.112	0.255	0.329
TS-1-0.60-443-144	86.2	65.3	390	0.110	0.267	0.317

[a)] S_{BET}: BET surface area; V_{micro}: micropore volume; V_{hollow}: volume of hollow cavities; I_{960}/I_{550}: the relative intensity of the absorption peaks at 960 and 550 $\mathrm{cm^{-1}}$ in the FTIR spectra.

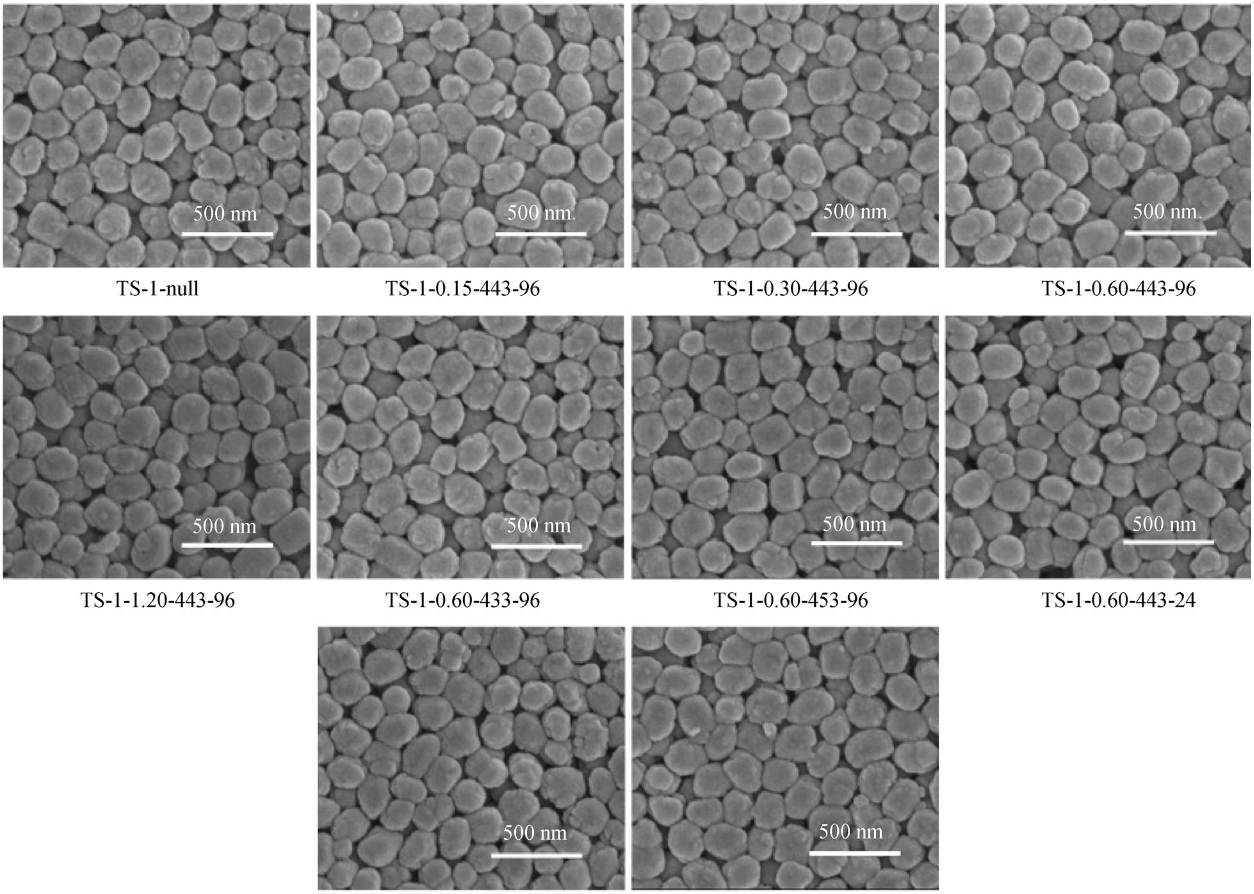

TS-1-null TS-1-0.15-443-96 TS-1-0.30-443-96 TS-1-0.60-443-96

TS-1-1.20-443-96 TS-1-0.60-433-96 TS-1-0.60-453-96 TS-1-0.60-443-24

TS-1-0.60-443-48 TS-1-0.60-443-144

Fig. 2 SEM images of TS-1 samples before and after TEA treatment

decrease of the BET specific surface areas and the increase of the volumes of the hollow cavities can be ascribed to the dissolution of TS-1 crystals in the basic solution.

It is seen that the V_{hollow} increases to varied extent with increasing the TEA concentrations. For example, with the increase of the TEA concentrations from 0.15 to 1.20 $\mathrm{mol \cdot L^{-1}}$, the V_{hollow} increases from 0.236 to 0.313 $\mathrm{cm^3 \cdot g^{-1}}$. It is also seen that the V_{hollow} increases with increasing the treatment temperature and time. For example, with increasing the treatment temperature from 433 to 443 K

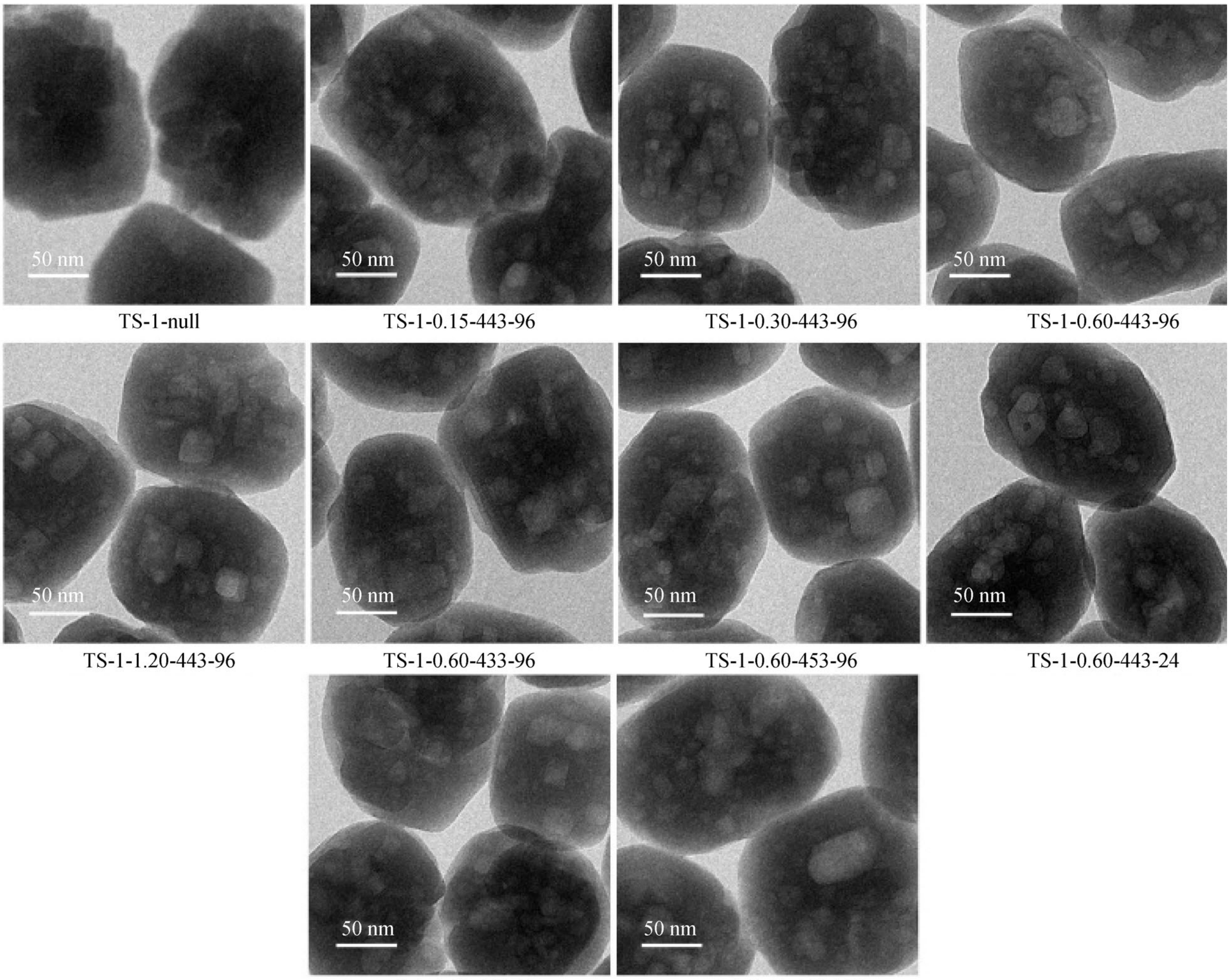

TS-1-null TS-1-0.15-443-96 TS-1-0.30-443-96 TS-1-0.60-443-96

TS-1-1.20-443-96 TS-1-0.60-433-96 TS-1-0.60-453-96 TS-1-0.60-443-24

TS-1-0.60-443-48 TS-1-0.60-443-144

Fig. 3 TEM images of TS-1 samples before and after TEA treatment

and then to 453 K, the V_{hollow} first increases remarkably from 0.256 to 0.265 $\text{cm}^3\cdot\text{g}^{-1}$, and then slightly to 0.268 $\text{cm}^3\cdot\text{g}^{-1}$. With the increase of the treatment time from 24 h to 96 h, the V_{hollow} increases from 0.248 to 0.265 $\text{m}^3\cdot\text{g}^{-1}$. However, the V_{hollow} increases slightly to 0.267 $\text{cm}^3\cdot\text{g}^{-1}$ with further increasing the treatment time to 144 h. The explanation for these phenomena is that the increase of the TEA concentrations, treatment temperature and treatment time lead to an increase of TS-1 dissolution in the TEA solution by desilication. The similar conclusions were reached on the treatment of TS-1 with NaOH in the literature [33].

The FTIR spectra of TS-1 samples before and after treatment are given in Fig. 5. All TS-1 samples show the adsorption bands around 550, 800, 960, 1100 and 1230 cm^{-1}, agreeing with the typical FTIR spectra of TS-1 in the literature [34]. The band at 550 cm^{-1} is assigned to the vibration of double five-membered ring unit and is considered as the fingerprint of the MFI structure. The band at 1230 cm^{-1} is attributed to asymmetrical stretching vibration of the MFI framework structure. The adsorption bands at 800 and 1100 cm^{-1} in the FTIR spectra are due to the symmetrical and antisymmetrical stretching vibration of [SiO_4] units respectively. The appearance of the band at 960 cm^{-1} is still controversial. It is believed that it is due to the stretching vibration of [SiO_4] units strongly influenced by titanium ions in neighboring coordination sites, which is a proof of the introduction of the Ti into the framework [35]. Indeed, a linear relationship between its intensity and the amounts of the framework titanium was found [36]. The relative intensity (I_{960}/I_{550}) of the absorption peaks at 960 and 550 cm^{-1} in the FTIR spectra was employed to exhibit the amounts of titanium in the framework [36,37]. The I_{960}/I_{550} values of all samples are given in Table 1. It can be seen that the I_{960}/I_{550} ratio decreases appreciably with increasing the TEA concentrations, e.g., from 0.15 to 1.2 $\text{mol}\cdot\text{L}^{-1}$, the ratio decreases from 0.343 to 0.302. However, the I_{960}/I_{550} ratio decreases slightly with increasing the treatment temperature and time, e.g., with the increase of treatment temperature from 433 to 453 K,

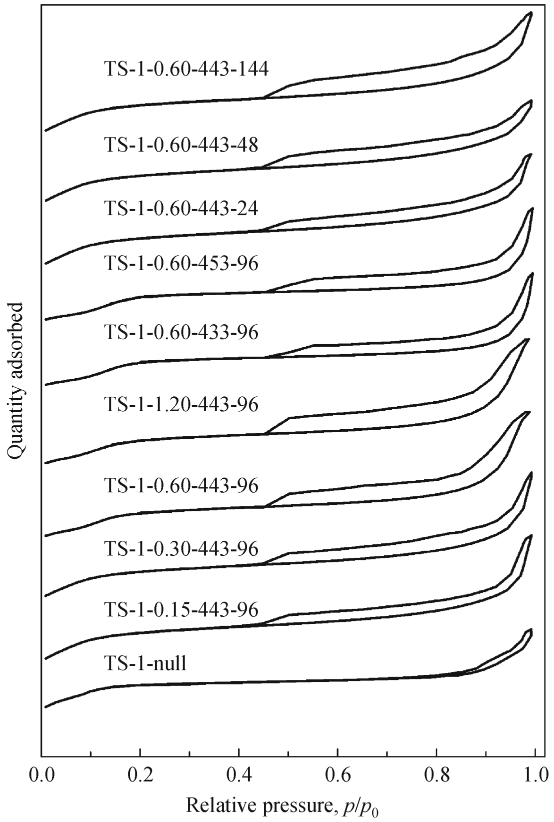

Fig. 4 N_2 adsorption/desorption isotherms for TS-1 samples before and after TEA treatment

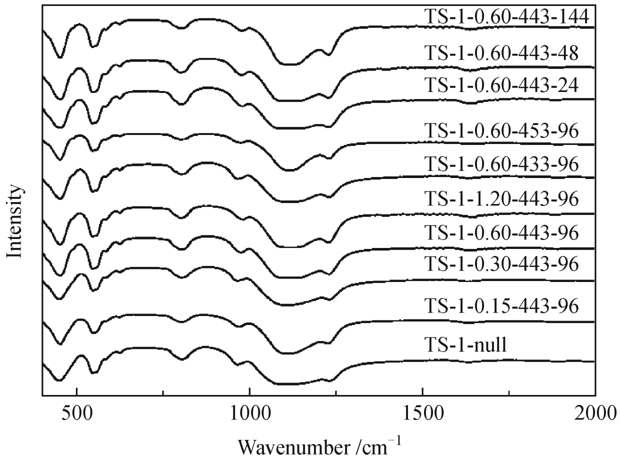

Fig. 5 FTIR spectra of TS-1 samples before and after TEA treatment

the I_{960}/I_{550} ratio decreases from 0.345 to 0.319, and with the increase of treatment time from 24 h to 144 h, it decreases from 0.347 to 0.317. These phenomena can be ascribed to the decrease of the amounts of the framework titanium, which is caused by the dissolution of silica in the TEA solution, but the titanium is deposited as titanium oxide.

UV-Vis spectroscopy is a common tool to determine the coordination of titanium ions in titanium-substituted zeolites. UV-Vis spectra of TS-1 samples before and after TEA treatment are presented in Fig. 6. It is clear that, all of the samples exhibit a strong band centered at 210 nm, characteristic of the isolated Ti^{4+} atoms in the tetrahedral coordination [38,39]. For all the treated samples, however, the absorption band at about 330 nm, which is considered as the existence of anatase TiO_2 [40], increases slightly in its intensity with increasing the treatment temperature and time, but increases appreciably with increasing the TEA concentration.

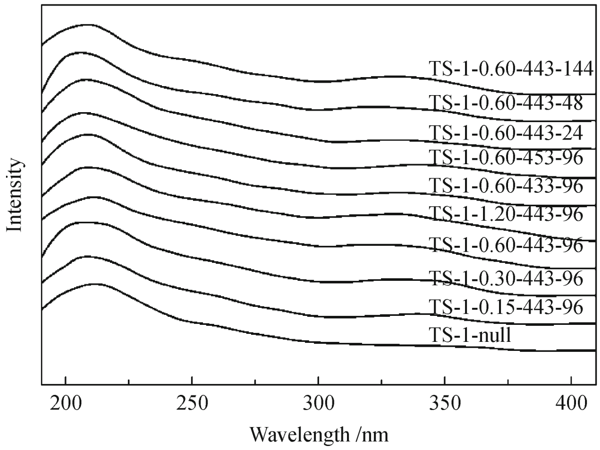

Fig. 6 UV-Vis spectra of TS-1 samples before and after TEA treatment

It was reported that the extra-framework Ti of the TS-1 samples treated by TPAOH decreased for the extra-framework Ti could be recrystallized into the framework of TS-1 [26,28]. However, the fallen framework titanium atoms, which are caused by the dissolution of silica during the TEA treatment, are hard to recrystallize into the framework because the TEA solution cannot structure-direct the synthesis of the MFI topology. So the anatase TiO_2 species are detected in the TS-1 samples after TEA treatment.

3.2 Effects of treatment conditions on the epoxidation of propylene

3.2.1 Effect of the TEA concentrations

TS-1 was treated at 443 K for 96 h with different concentrations of TEA (0.15, 0.3, 0.6, and 1.2 mol·L^{-1}). The catalytic properties of these TS-1 samples and TS-1-null for the epoxidation of propylene were studied, and the results are shown in Fig. 7. It can be seen that the catalyst lives of all the treated TS-1 samples increase markedly compared with that of TS-1-null (27 h). The catalyst life increases from 40 h to 53 h by increasing the TEA concentrations from 0.15 to 0.6 mol·L^{-1} but decreases to 49 h with further increasing the TEA concentration to 1.2 mol·L^{-1}.

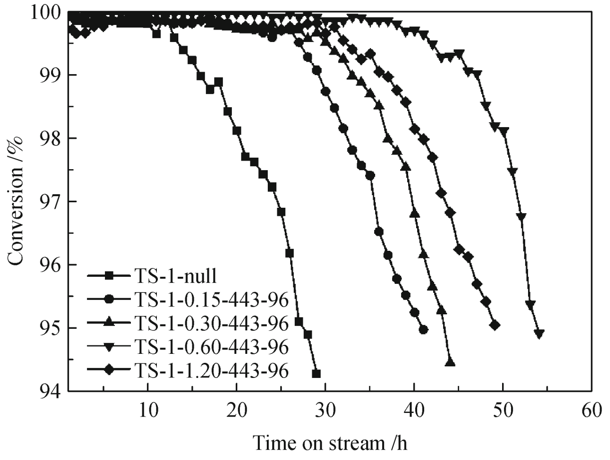

Fig. 7 Effect of TEA concentrations on the epoxidation of propylene. Reaction conditions: T = 323 K, P = 2.5 MPa, 3.00 g catalysts, 0.67 cm^3·s^{-1} N_2, CH_3OH : H_2O_2 : C_3H_6 : H_2O = 6.44 : 1 : 3.06 : 6.29 (mol), weight hourly space velocity (WHSV) of H_2O_2 = 0.67 h^{-1}

3.2.2 Effect of TEA treatment temperature

Figure 8 presents the influence of the treatment temperature (433, 443 and 453 K) on the epoxidation of propylene, at the TEA concentration of 0.6 mol·L^{-1} for 96 h. It can be seen that the catalyst life increases with the increase of the treatment temperature, e.g., with increasing the treatment temperature from 433 to 443 K and then to 453 K, the catalyst life first increases significantly from 41 to 53 h, and then slightly to 54 h. It has been known from above that catalyst life is greatly affected by the volumes of the hollow cavities. With increasing the treatment temperature from 433 to 443 K, the volume of the hollow cavities increases remarkably, while it increases slightly to 453 K, so the catalyst lives exhibit the same trend.

3.2.3 Effect of TEA treatment time

TS-1 was treated at 443 K for different hours (24, 48, 96 and 144 h), at the TEA concentration of 0.6 mol·L^{-1} . The properties of the obtained catalysts for the epoxidation of propylene are shown in Fig. 9. It can be seen that the catalyst life increases with increasing the treatment time. The catalyst life of TS-1 treated for 24 h is 42 h. With the increase of treatment time to 96 h, the catalyst life is appreciably prolonged to 53 h. However, the catalyst life

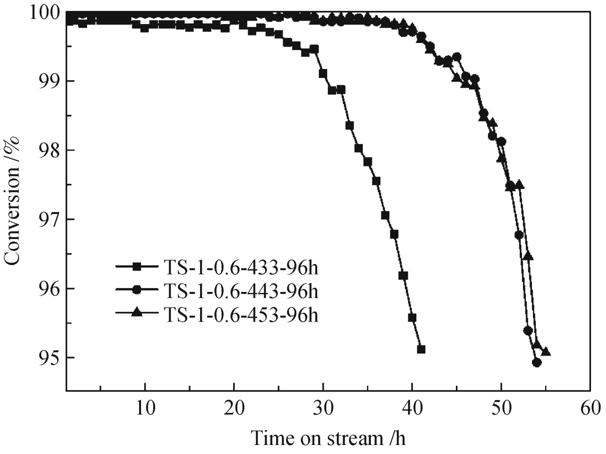

Fig. 8 Effect of TEA treatment temperature on the epoxidation of propylene. Reaction conditions: T = 323 K, P = 2.5 MPa, 3.00 g catalysts, 0.67 cm^3·s^{-1} N_2, CH_3OH : H_2O_2 : C_3H_6 : H_2O = 6.44 : 1: 3.06 : 6.29 (mol), WHSV(H_2O_2) = 0.67 h^{-1}

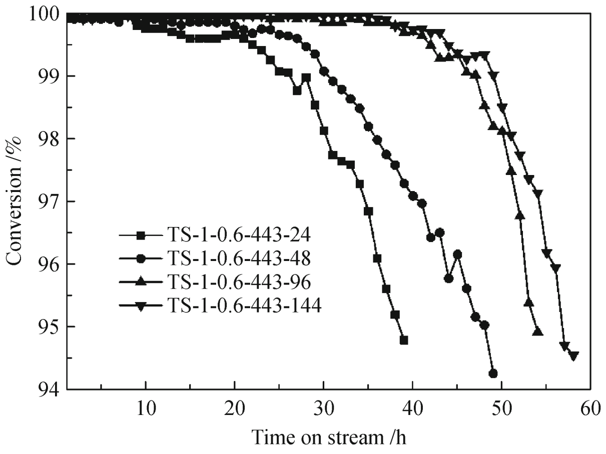

Fig. 9 Effect of TEA treatment time on the epoxidation of propylene. Reaction conditions: T = 323 K, P = 2.5 MPa, 3.00 g catalysts, 0.67 cm^3·s^{-1} N_2, CH_3OH : H_2O_2 : C_3H_6 : H_2O = 6.44 : 1: 3.06 : 6.29 (mol), WHSV(H_2O_2) = 0.67 h^{-1}

increases slightly to 55 h with further increasing the treatment time to 144 h. With increasing the treatment time, more hollow cavities are created in the crystals and the volumes of the hollow cavities increase, so the catalyst life increases. It has been known that TS-1-0.6-443-144 has a similar volume of hollow cavities with TS-1-0.6-443-96, so that these two samples exhibit the similar catalytic stability.

The mechanism behind the excellent catalytic performance of TS-1 can be explained using Scheme 1, as reported by Clerici [41]. In the reaction media, an equilibrium exists between methanol solvent and hydrogen

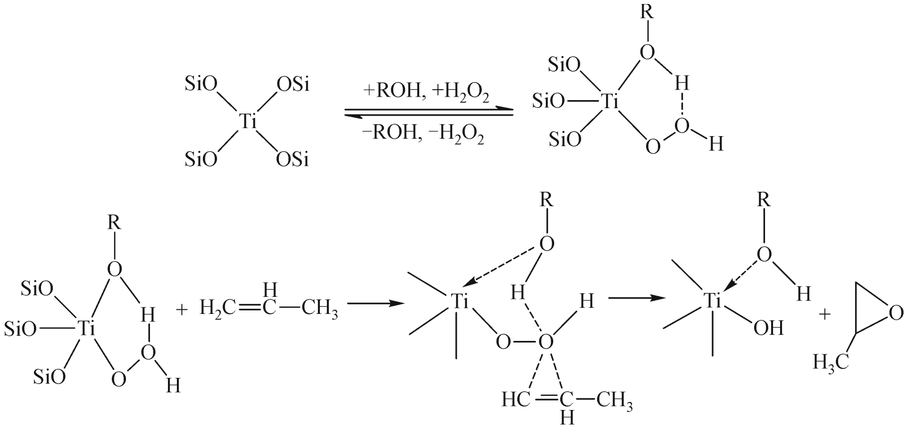

Scheme 1 Catalytic mechanism of titanium silicalite-1

peroxide. The Ti-OOH species, which is formed by the interaction between the Ti atom framework and the H_2O_2 molecule, can form a stable five-membered cyclic structure with a hydroxyl moiety coordinated on Ti. The stable five-membered cyclic structure then reacts with propylene to form PO on the active sites, which are suited in a channel system of about 0.55 nm average diameter. However, the repeated catalyzed reaction of by-products with PO leads to the formation of small amounts of propylene oxide oligomers within the TS-1 micropores. With increasing the chain length, the diffusivity of these oligomers decreases rapidly, until they literally get stuck in the TS-1 pores to block the access of the reactants to the catalytic centers and thus deactivate the catalyst [42]. Because the characterization results show that only the hollow cavities have been created after the TEA treatment, it should be these cavities to lead to the increase of the catalyst life in propylene epoxidation. With large hollow cavities, the reactants can diffuse into TS-1 more conveniently, the resistance of the products diffusing out of TS-1 decreases, and more propylene oxide oligomers can be removed. As the hollow cavities are filled with the oligomers, the catalyst activity decreases gradually. However, the hollow cavities are not the larger the better for the reaction. A large volume of the hollow cavities means a heavy damage to the TS-1 crystals and a considerable loss of the framework Ti species, which has been demonstrated by the FTIR and UV-Vis results.

4 Conclusions

In conclusion, a lot of hollow cavities are created in the TS-1 crystals treated with TEA. The volume of the hollow cavities increases with increasing the TEA concentrations, treatment temperature and time. Compared with TS-1-null, the catalyst lives of all the treated TS-1 samples are improved in the epoxidation of propylene due to the generation of the hollow cavities. With the increase of the concentrations of TEA, the catalyst life first increases and then decreases. With increasing the treatment temperature and time, the volume of the hollow cavities first increases obviously and then slightly, so the catalyst life exhibits the same trend. After the treatment, TEA can be separated from the treatment solution through distillation and recycled. The results in this work would be useful for the industrial production of propylene oxide.

Acknowledgements This work was supported by National Natural Science Foundation of China (Grant No. 21276183).

References

1. Valbert J R, Zajacek J G, Orenbuch D. Encyclopedia of Chemical Processing and Design. New York: American Library Association Press, 1993, 88
2. Nijhuis T A, Makkee M, Moulijn J A, Weckhuysen B M. The production of propene oxide: Catalytic process and recent development. Industrial & Engineering Chemistry Research, 2006, 45(10): 3447–3459
3. Wang L N, Wang Y Q, Wu G Q, Feng W P, Zhang T, Yang R M, Jin X, Shi H N, Wang S H. Epoxidation of propylene over Titanosilicate-1 in fixed-bed reactor: Experiment and Kinetics. Asian Journal of Chemistry, 2014, 26(4): 943–950
4. Taramasso M, Perego G, Notari B. U S. Patent, 4410501, 1983–07–12
5. Peregot G, Bellussi G, Corno C, Taramasso M, Buonomot F, Esposito A. New developments in zeolite science and technology. Studies in Surface Science and Catalysis, 1986, 28: 129–136
6. Bhaumik A. Tatsumi1 T. Selective dihydroxylation over titanium silicate molecular sieves. Journal of Catalysis, 1998, 176(2): 305–309
7. Mukherjee P, Bhaumik A, Kumar R. Eco-friendly, selective hydroxylation of C-7 aromatic compounds catalyzed by TS-1/

H_2O_2 system under solvent-free solid-liquid-liquid-type triphase conditions. Industrial & Engineering Chemistry Research, 2007, 46 (25): 8657–8664

8. Sheldon R A, Downing R S. Heterogeneous catalytic transformation for environmentally friendly production. Applied Catalysis A, General, 1999, 189(2): 163–183
9. Corma A, Garcia H. Lewis acids as catalysts in oxidation reactions: From homogeneous to heterogeneous systems. Chemical Reviews, 2002, 102(10): 3837–3892
10. Kong L Y, Li G, Wang X S. Kinetics and mechanism of liquid-phase oxidation of thiophene over TS-1 using H_2O_2 under mild conditions. Catalysis Letters, 2004, 92(3–4): 163–167
11. Wang X X, Li G, Wang W H, Jin C Z, Chen Y Y. Synthesis, characterization and catalytic performance of hierarchical TS-1 with carbon template from sucrose carbonization. Microporous and Mesoporous Materials, 2011, 142(2-3): 494–502
12. Clerici M G, Bellussi G, Romano U. Synthesis of propylene oxide from propylene and hydrogen peroxide catalyzed by titanium silicalite. Journal of Catalysis, 1991, 129(1): 159–167
13. Thiele G F, Roland E. Propylene epoxidation with hydrogen peroxide and titanium silicalite catalyst: Activity, deactivation and regeneration of the catalyst. Journal of Molecular Catalysis, 1997, 117(1-3): 351–356
14. Tuel A. Crystallization of titanium silicalite-1 from gels containing hexanediamine and tetrapropylammonium bromide. Zeolites, 1996, 16(2-3): 108–117
15. Wang X S, Guo X W, Li G. Synthesis of titanium silicalite from the TPABr system and its catalytic properties for epoxidation of propylene. Catalysis Today, 2002, 74(1-2): 65–75
16. Liz W. HPPO plant for Antwerp. Urethane Technology, 2004, 21(5): 4
17. Perego C, Carati A, Ingallina P, Mantegazza M A, Bellussi G. Production of titanium containing molecular sieves and their application in catalysis. Applied Catalysis A, General, 2001, 221 (1-2): 63–72
18. Li C Y, Shen B X, Zhao J G. Effect of propylene glycol monomethyl ether and rust impurities on TS-1 deactivation in propylene epoxidation. Catalysis Today, 2013, 212: 169–174
19. Zuo Y, Song W, Dai C, He Y, Wang M, Wang X, Guo X. Modification of small-crystal titanium silicalite-1 with organic bases: Recrystallization and catalytic properties in hydroxylation of phenol. Applied Catalysis A, General, 2013, 453: 272–279
20. Tao Y, Kanoh H, Abrams L, Kaneko K. Mesopore-modified zeolites: Preparation, characterization and applications. Chemical Reviews, 2006, 106(3): 896–910
21. Wang Y, Tuel A. Naniporous zeolite single crystals: ZSM-5 nanoboxed with uniform intracrystalline hollow structure. Microporous and Mesoporous Materials, 2008, 113(1-3): 286–295
22. Groen J C, Peffer A A, Moulijin J A, Pérez-Ramírez J. On the introduction of intracrystalline mesoporosity in zeolites upon desilication in alkaline medium. Microporous and Mesoporous Materials, 2004, 69(1-2): 29–34
23. Silvestre-Albero A, Grau-Atienza A, Serrano E, García-Martínez J, Silvestre-Albero J. Desilication of TS-1 zeolite for the oxidation of bulky molecules. Catalysis Communications, 2014, 44: 35–39
24. Lin M, Shu X, Wang X, Zhu B. U S. Patent, 6475465, 2002
25. Lin M, Zhu B, Shu X T, Wang X Q. The development and application of hierarchical titanium silicalite-1. Petrochemical Technology, 2005, 34: 377–379
26. Wang Y, Lin M, Tuel A. Hollow TS-1 crystals formed via a dissolution recrystallization process. Microporous and Mesoporous Materials, 2007, 102(1-3): 80–85
27. Tsai S, Chao P, Tsai T, Wang I, Liu X, Guo X. Effect of pore structure of post-treated TS-1 on phenol hydroxylation. Catalysis Today, 2009, 148(1-2): 174–178
28. Lin J, Xin F, Yang L, Zhuang Z. Synthesis, charactrtization of hierarchical TS-1 and its catalytic performance for cyclohexanone ammoximation. Catalysis Communications, 2014, 45: 104–108
29. Wu G Q, Wang Y Q, Wang L N, Feng W P, Shi H N, Lin Y, Zhang T, Jin X, Wang S H, Wu X X, Yao P X. Epoxidation of propylene with H_2O_2 catalyzed by supported TS-1 catalyst in a fixed-bed reactor: Experiments and kinetics. Chemical Engineering Journal, 2013, 215-216: 306–314
30. Clerici M G, Ingallina P. Epoxidation of lower olefins with hydrogen peroxide and titanium silicalite. Journal of Catalysis, 1993, 140(1): 71–83
31. Wang X B, Zhang X, Liu H, Yeung K L, Wang J. Preparation of titanium silicalite-1 catalytic films and application as catalytic membrane reactor. Chemical Engineering Journal, 2010, 156(3): 562–570
32. Serrano D P, Sanz R, Pizarro P, Moreno I. Nanosized gold-catalyed selective oxidation of alkyl-substituted benzenes and *n*-alkanes. Applied Catalysis A, General, 2012, 435-436: 32–42
33. Groen J C, Moulijn J A, Pérez-Ramírez J. Alkaline posttreatment of MFI zeolite. From accelerated screening to scale-up. Industrial & Engineering Chemistry Research, 2007, 46(12): 4193–4201
34. Fejes P, Nagy J B, Halász J, Oszkó A. Heat-treatment of isomorphously substituted ZSM-5 zeolites and its structural consequences: An X-ray diffraction, ^{29}Si Mas-NMR, XPS and FTIR spectroscopy study. Applied Catalysis A, General, 1998, 175 (1-2): 89–104
35. Ricchiardi G, Damin A, Bordiga S, Lamberti C, Spanò G, Rivetti F, Zecchina A. Vibrational structure of titanium silicate catalysts: A spectroscopic and theoretical study. Journal of the American Chemical Society, 2001, 123(46): 11409–11419
36. Thangaraj A, Kumar R, Mirajkar S P, Ratnasamy P. Catalytic properties of crystalline titanium silicalite-1: Synthesis and characterization of titanium-rich zeolites with MFI structure. Journal of Catalysis, 1991, 130(1): 1–8
37. Tatsumi T, Jappar N. Ammoximation of cyclic ketones on TS-1 and Amorphous SiO_2-TiO_2. Journal of Catalysis, 1996, 161(2): 570–576
38. Serrano D P, Calleja G, Botas J A, Gutierrez F J. Characterization of adsorption and hydrophobic properties of siliacalite-1, ZSM-5, TS-1 and Beta zeolites by TPD Techniques. Separation and Purification Technology, 2007, 54(1): 1–9
39. On D T, Kaliaguine S, Bonneviot L. Titanium boralites with MFI structure characterized XRD, XANES, IR and UV-Visible techniques: Effect of hydrogen peroxide on the preparation. Journal of Catalysis, 1995, 157(1): 235–243
40. Deng X J, Wang Y N, Shen L, Wu H H, Liu Y M, He M Y. Low-cost

synthesis of titanium silicalite-1 with highly catalytic oxidation performance through a controlled hydrolysis process. Industrial & Engineering Chemistry Research, 2013, 52(3): 1190–1196

41. Clerici M G, Bellussi G, Romano U. Synthesis of propylene oxide from propylene and hydrogen peroxide catalyzed by titanium silicalite. Journal of Catalysis, 1991, 129(1): 159–167
42. Wang Q F, Wang L, Chen J X, Wu Y L, Mi Z T. Deactivation and regeneration of titanium silicalite catalyst for epoxidation of propylene. Journal of Molecule Catalysis A, Chemical, 2007, 273 (1-2): 73–80